

# Short Distance Current Correlators: Comparing Lattice Simulations to the Instanton Liquid

Thomas DeGrand

*Department of Physics, University of Colorado, Boulder, CO 80309 USA*

(October 29, 2018)

Point to point correlators of currents are computed in quenched QCD using a chiral lattice fermion action, the overlap action. I compare correlators made of exact quark propagators with correlators restricted to low (less than 500 MeV) eigenvalue eigenmodes of the Dirac operator. In many cases they show qualitative resemblance (typically at small values of the quark mass and distances larger than 0.4 fm) and they differ qualitatively at larger quark masses or at very short distance. Lattice results are in qualitative agreement (and in the difference of vector and axial vector channels, quantitative agreement) with the expectations of instanton liquid models. The scalar channel shows the effects of a quenched finite volume zero mode artifact, a negative correlator.

## I. INTRODUCTION

One of the earliest attempts to study nonperturbative behavior in QCD was through an analysis of correlators of hadronic currents. The QCD sum rule approach treats short distance physics in the context of the operator product expansion (OPE) and parameterizes long distance physics in terms of vacuum condensates [1,2]. The approach was quite successful in the vector and axial vector channels, but nonperturbative effects are very large in the pseudoscalar and scalar channels. The realization that instanton effects appear in precisely those channels in which nonperturbative effects are large led to the development of instanton liquid models [3,4]. It would be an interesting exercise to “validate” the parameterization and results of these models directly from the QCD Lagrangian, by using lattice methods. This paper is a step in that direction.

We are concerned with flavor non-singlet current correlators separated by a (four dimensional Euclidean) distance  $x$ ,

$$\Pi_i(x) = \text{Tr}\langle J_i^a(x)J_i^a(0)\rangle \quad (1)$$

where the current will be proportional to

$$J_i^a(x) = \bar{\psi}(x)\tau^a\Gamma(i)\psi(x) \quad (2)$$

with  $\tau^a$  an isospin label and  $\Gamma$  a product of Dirac matrices. In practice (and to be consistent with the standard approach to these correlation functions [5]) I present results for the correlators scaled with respect to the massless free field current-current correlator  $\Pi_i^0(x)$  (the precise kind of free fermions will be described below)

$$R_i(x) = \Pi_i(x)/\Pi_i^0(x). \quad (3)$$

The label  $i$  will include the pseudoscalar (PS), scalar (S), vector (V) and axial vector (A) currents.

The Euclidean space correlators whose Fourier transforms into coordinate space I am measuring obey a dispersion relation which relates them to their absorptive part in Minkowski space, the spectral density  $\rho(s)$ ,

$$\Pi(q^2) = \frac{1}{\pi} \int ds \frac{\rho(s)}{s + q^2}. \quad (4)$$

$\rho(s)$  is in turn is proportional to the total cross section for scattering in the appropriate channel, and should then be positive. The point-to-point correlators measured here are then related to the spectral density through

$$\Pi(x) = \int d^4q \exp(iq \cdot x) \frac{1}{\pi} \int ds \frac{\rho(s)}{s + q^2} \quad (5)$$

or, more directly,

$$\Pi(x) = \frac{1}{\pi} \int ds \rho(s) D(\sqrt{s}, |x|) \quad (6)$$

where

$$D(\sqrt{s}, |x|) = \frac{1}{4\pi^2} \int_0^\infty \frac{p^2 dp}{\sqrt{p^2 + s}} \exp(-|x| \sqrt{p^2 + s}) \quad (7)$$

is the Euclidean propagator for a free particle of squared mass  $s$ . If we were measuring a conventional (for the lattice)  $\vec{q} = 0$  correlator, Eq. 7 would be replaced by

$$D_{\vec{q}=0}(m, |x|) = \frac{\exp(-m|x|)}{2m}. \quad (8)$$

In principle, lattice calculations could check results of instanton liquid models [5]. In practice, however, lattice simulations have been contaminated by the use of fermion actions which are not chiral. Since the continuum analyses depend crucially on chiral symmetry arguments, one might wish to be cautious about drawing conclusions from simulations with nonchiral lattice fermions. The recent discovery of lattice actions which support an exact chiral symmetry [6] (notably the overlap action [7]) allows one to revisit these questions in a theoretically clean context. That is the subject of this paper: a study of current correlators from an overlap fermion action.

Because I am working with an action with exact chiral symmetry, I have to be careful with my definitions and make them consistent with current commutation relations. If I assume that I am modeling a theory with a flavor  $SU(2)_V \times SU(2)_A \simeq O(4)$  symmetry, I can write down two real  $O(4)$  vectors of currents

$$\vec{\phi}_1 = (\pi^a, f_0) \quad (9)$$

and

$$\vec{\phi}_2 = (a_0^a, \eta) \quad (10)$$

where  $\pi^a = i\bar{\psi}\gamma_5(\tau^a)\psi \equiv J_{PS}$  is the pseudoscalar (PS) current,  $a_0^a = -\bar{\psi}(\tau^a/2)\psi \equiv J_S$  is the scalar (S) isotriplet current,  $f_0 = \bar{\psi}\psi$  is the scalar isoscalar current, and  $\eta = i\bar{\psi}\gamma_5\psi$  is the pseudoscalar isoscalar current. (Correlators of the last two currents involve disconnected diagrams and I will not consider them further.)

In the cases of the V (vector) ( $\Gamma = \gamma_\mu$ ), and A (axial vector) ( $\Gamma = \gamma_\mu\gamma_5$ ) currents, I sum the correlator over the four values of  $\mu$ . The most interesting way to present results for correlators in the vector and axial vector channels is to look at the sum or difference of vector and axial vector correlators

$$R_{V\pm A}(x) = \frac{\Pi_V(x) \pm \Pi_A(x)}{2\Pi_V^0(x)}. \quad (11)$$

In the sum rule/OPE approach  $R_{V+A}$  is dominated by perturbative physics and is expected to take a value very close to unity, while  $R_{V-A}$  is zero at small  $x$  and receives only nonperturbative contributions which are relevant to chiral symmetry breaking. The instanton liquid model produces a large part of the correlator  $R_{V-A}$ , as emphasized recently by Schafer and Shuryak [8].

In a recent publication [9] we have shown that the low lying eigenmodes of a chiral lattice fermion Dirac operator, an overlap fermion operator (described in Ref. [10]), has a local chiral density  $\psi(x)^\dagger \gamma_5 \psi(x)$  which shows a peaked structure. The positions and signs of the peaks are strongly correlated with the locations of topological objects, which would be identified as instantons and anti-instantons detected using a pure gauge operator. Zero modes correlate with only one sign of topological objects, while nonzero eigenmodes of the Dirac operator interpolate between both signs of topological object. This correlation dies away slowly as the eigenvalue of the mode rises. Spatially averaged correlation functions of hadrons made of light quarks are saturated by propagators of quarks restricted to a few low eigenmodes. The whole picture is very reminiscent of an instanton liquid model.

Ref. [9] did not consider the possibility that the density of the fermionic modes might be large in places where the local chiral density was small. Subsequently, this point was raised by the authors of Ref. [11]. Ref. [12] showed that this possibility did in fact not occur for the overlap action used in Ref. [9]. Similar results have been presented using an alternative chiral lattice action (the Wilson overlap action) [13] two lattice actions with improved but inexact chiral symmetry (domain wall fermions [14] and an approximate Ginsparg-Wilson action [15]) and with an improved operator in a lattice action with inexact chiral symmetry (the clover action) [16]. None of these last three works compared the distribution of chirality with topological charge density measured with a gauge observable.

It is an uncontrolled approximation to replace a quark propagator by the quark propagator restricted to a sum over a small number of small eigenvalue eigenmodes of the Dirac operator. However, if an observable computed with truncated propagators resembles the same observable computed with exact propagators, and if we further have seen that the low modes couple to particular structures in the QCD vacuum, then this resemblance is a strong (qualitative) signal that the particular vacuum structure is connected with that observable.

For example, consider the difference of vector and axial vector currents.  $R_{V-A}(x)$ , either extracted from  $\tau$ -decay or measured in Monte Carlo simulation, is zero at small  $x$  and increases with  $x$ . The same behavior is seen in a calculation based on propagators truncated to a small number of eigenmodes: in fact, at small quark mass (pseudoscalar to vector mass ratio less than 0.5) the difference between the exact and truncated  $R_{V-A}(x)$  is small. Since in [9] the locations of peaks in the low eigenvalue modes were correlated with the locations of peaks in the topological charge density, one can infer that instantons are connected with the rise in  $R_{V-A}(x)$ .

If the current correlator based on truncated propagators does not reproduce the full calculation, the truncated propagator must be missing some important physics. For example, in most channels,  $R(x)$  approaches unity as  $x$  falls to zero. Approximating quark propagators by a few low eigenvalue modes does not reproduce this behavior: in that case  $R(x)$  typically vanishes at small  $x$ . Presumably  $R(x) \rightarrow 1$  as  $x \rightarrow 0$  is asymptotic freedom at work: the correlator is reducing to its free-field value. The low eigenmodes are extended in space and decouple from short distance physics.

Previous studies [17,18] of point-to-point correlators have mostly been concerned with the long-distance behavior of these observables, including the extraction of particle masses and couplings. I will not attempt to do that here, because my simulation volume is very small. Some studies [19] have also compared the correlators in a “full” QCD simulation with propagators truncated to a set of low-eigenvalue eigenmodes. They see results similar to the ones I report, the main difference being that they need many more eigenmodes to saturate the correlator. I believe that this difference is due to the poor chiral behavior of the action, the usual thin link Wilson action, used by these authors.

Along the way, I observe an interesting artifact of the quenched approximation in the scalar channel—the correlation function becomes negative. This behavior is incompatible with a normal spectral representation. In my data it seems to be associated with a finite-volume quenched approximation artifact arising from the exact zero modes of the Dirac operator.

## II. THE LATTICE CALCULATION

The overlap action used in these studies [10] is built from an action with nearest and next-nearest neighbor couplings, and APE-blocked links [20]. Eigenmodes of the massless overlap Dirac operator  $D(0)$  are constructed from eigenmodes of the Hermitian Dirac operator  $H(0) = \gamma_5 D(0)$ , using an adaptation of a Conjugate Gradient algorithm of Bunk et. al. and Kalkreuter and Simma [21]. These eigenmodes are used to precondition the calculation of the quark propagator (by use of a conjugate gradient algorithm) and are additionally used to construct quark propagators truncated to some number of low lying eigenmodes.

Later, we will need a few simple facts about the eigenmodes of the overlap Dirac operator, so let us recall them now. The eigenmodes of any massless overlap operator are located on a circle in the complex plane of radius  $x_0$  with a center at the point  $(x_0, 0)$ . The corresponding eigenfunctions are either chiral (for the eigenmodes with real eigenvalues located at  $\lambda = 0$  or  $\lambda = 2x_0$ ) or nonchiral and paired; the two eigenvalues of the nonchiral modes are complex conjugates. The massive overlap Dirac operator is conventionally defined to be

$$D(m) = \left(1 - \frac{m}{2x_0}\right)D(0) + m \quad (12)$$

and it is also conventional to define the propagator so that the chiral modes at  $\lambda = 2x_0$  are projected out,

$$\hat{D}^{-1}(m) = \frac{1}{1 - m/(2x_0)} \left(D^{-1}(m) - \frac{1}{2x_0}\right). \quad (13)$$

Then the contribution to the propagator of a single (positive chirality) zero mode in the basis where  $\gamma_5 = \text{diag}(1, -1)$  is

$$\hat{D}(m)^{-1} = \frac{1}{m} \begin{pmatrix} 1 & 0 \\ 0 & 0 \end{pmatrix}. \quad (14)$$

The  $j$ th pair of nonchiral modes contributes a term

$$\hat{D}(m)_j^{-1} = \begin{pmatrix} \alpha_j & -\beta_j \\ \beta_j & \alpha_j \end{pmatrix}, \quad (15)$$

where, defining  $\mu = m/(2x_0)$ ,  $\epsilon_j = \lambda_j/(2x_0)$ , the entries are

$$\alpha_j = \frac{1}{2x_0} \frac{\mu(1 - \epsilon_j^2)}{\epsilon_j^2 + \mu^2(1 - \epsilon_j^2)} \quad (16)$$

$$\beta_j = \frac{1}{2x_0} \frac{\epsilon_j \sqrt{1 - \epsilon_j^2}}{\epsilon_j^2 + \mu^2(1 - \epsilon_j^2)} \quad (17)$$

and  $D(0)^2 \phi_j = \lambda_j^2 \phi_j$ ; the eigenmodes of  $D(0)$  have eigenvalues  $2x_0(\epsilon_j^2 \pm i\epsilon_j \sqrt{1 - \epsilon_j^2})$ . For a summary of these useful formulas, see Ref. [22] (for the special case  $x_0 = 1/2$ ).

The data set used in this analysis are generated in quenched approximation using the Wilson gauge action at a coupling  $\beta = 5.9$ . The nominal lattice spacing is  $a = 0.11$  (inferred from the Sommer parameter using the interpolation formula of Ref. [23]) or 0.13 fm from the rho mass. This will be discussed in more detail below. It consists of 20  $12^4$  configurations. The fermions have periodic boundary conditions in the spatial directions and anti-periodic temporal boundary conditions. I calculated the ten smallest eigenvalue modes of  $H^2(0)$  in the chiral sector of the minimum eigenvalue, and reconstructed the degenerate eigenstate of opposite chirality of  $H^2(0)$  when one was present. These modes are then recoupled into eigenmodes of  $D(0)$ . Their eigenvalues have imaginary parts ranging up to  $0.3/a - 0.35/a$ , or about 500 MeV [9].

The lattice analysis has one strong point and one weak point. The strong point is the use of an action with exact chiral symmetry. This means that there is no additive renormalization of the quark mass. It also means that there are no exceptional configurations, so the simulations can be performed at small quark mass. Instead of exceptional configurations, there are contributions to the quark propagator from zero modes of the Dirac operator. Because of chiral symmetry, these zero modes contribute in a “dangerous” way, as finite volume effects only in the PS and S channels. The particular choice of action, with a fat link, also has rather mild multiplicative renormalization of current matrix elements. The perturbation theory has not been done for this action, but similar calculations done for the fat link clover action have vector and axial vector lattice-to-continuum renormalization factors quite close to unity [24].

The weak point of the calculation is its use of a small volume. The lattice has a size of about 1.5 fm, assuming a lattice spacing of 0.13 fm.

One annoyance encountered in this study is the different finite volume effects suffered by the free massless current correlator and the correlator in the nontrivial gauge background. At large distance the free correlator can receive contributions in which the quark and antiquark wind in opposite directions around the lattice, so that the correlator has the topology of a single line encircling the simulation volume. This contribution is not present in the nontrivial background, since it corresponds to a single Polyakov loop winding around the lattice. Confinement forces the expectation value of this operator to be zero. The way I got around this problem is the same as was used in Ref. [17]:

Think of the finite volume lattice as a piece of an infinite lattice. A propagator from a point source in the finite lattice corresponds, on the infinite lattice, to a sum of propagators from sources which include the original source, plus a set of image points on all the “copies” of the finite lattice which tile the infinite lattice. We only want to include contributions to correlators from infinite-volume propagators where the source points for the quark propagator and antiquark propagator coincide, and so do the sink points. These quark-antiquark correlators look like closed fermion loops. Contributions in the finite volume in which the quark and antiquark propagate in opposite directions around the finite volume to get to the same sink point are topologically equivalent to lines in the infinite volume, where the quark source and antiquark source sit on different image points and the two propagators terminate on the same sink point.

To compute the necessary free field current-current correlator, I construct an approximation to the infinite volume free fermion propagator by computing the free (overlap) fermion propagator on a large lattice (I used a  $24^4$  volume) and approximate the quark-antiquark correlators in the small volume as a sum of the “direct” term and propagators from sources located on (the same) nearest image point.

The hadron correlators also suffer finite volume effects. In particular, the lattice volume cuts off the long distance part of the hadron correlator, which in most cases contains the contribution to the correlator of the lightest state in the channel. Thus, I have not tried to do any fits to the mass of this state, in contrast to Refs. [17,18]. Note however, that for short distances (less than 0.5 fm or so), the effects of finite volume are not too important. Also, comparisons of a full correlator to a correlator computed using truncated propagators are not affected by the free field correlators, so the observation that low modes saturate a correlator (or not) are not so compromised.

At very light quark mass, chiral symmetry breaking begins to be modified by the small volume. The relevant parameter is the Leutwyler-Smilga [25] parameter,  $z = m_q \Sigma V$  for quark mass  $m_q$ , infinite volume condensate  $\Sigma = \langle \bar{q}q \rangle$ ,

and simulation volume  $V$ . A large volume corresponds to  $z \gg 1$ . Using the value of  $\Sigma$  computed for this action at this coupling in Ref. [10],  $z \simeq 0.8(am_q/0.01)$  (to show  $z$  in units of the smallest quark mass used). At this quark mass the scaled lattice size  $L$  is  $m_\pi L \simeq 2.4$ .

### III. RESULTS

#### A. The pseudoscalar and scalar channels

In Fig. 1 is shown the pseudoscalar correlator for several choices of light quark masses, with pseudoscalar to vector meson mass ratios ( $m_{PS}/m_V$ ) inferred from Ref. [9]: (a)  $am_q = 0.01$  ( $m_{PS}/m_V \simeq 0.34$ ); (b)  $am_q = 0.02$  ( $m_{PS}/m_V \simeq 0.50$ ); (c)  $am_q = 0.04$  ( $m_{PS}/m_V \simeq 0.61$ ); (d)  $am_q = 0.06$  ( $m_{PS}/m_V \simeq 0.64$ ). The separation  $x$  is measured in units of the lattice spacing in the simulation. Also shown is the contribution to the correlator from the lowest ten modes of the Dirac operator, as well as the contribution to the correlator given by the zero modes alone. Quark interactions in this channel are strongly attractive. The enormous attraction in the pseudoscalar channel is well known in continuum (compare Ref. [26]) and lattice (compare Ref. [17]) analyses. In instanton liquid phenomenology it is ascribed to the effect of the 't Hooft interaction, which is strong and attractive in the pseudoscalar channel. At low quark masses ( $m_{PV}/m_V \leq 0.5$  or so) the low mode truncation saturates the correlator at larger  $x$ . As these are the modes which couple to instantons, there seems to be a connection between instantons and the strong attraction in the pseudoscalar channel at  $x/a = 5 - 9$ .

The fact that the contribution of the low modes begins at  $R(x=0) = 0$  and not 1 is just a sign that at tiny  $x$  the channel is dominated by free-field modes (which presumably do not couple to topology), but by a distance of 2-4 lattice spacings (0.2-0.4 fm) the light quark mass correlator is completely dominated by the low modes. As the quark mass falls to zero, the pure zero modes make an ever larger contribution to the point-to-point correlators, as well: their contribution scales a  $1/m_q^2$  times a quark-mass-independent function of  $x$  and  $y$ ,

$$\Pi^{zero}(x, y) = \frac{1}{m_q^2} \left| \sum_{j \in zero} \phi_j(x) \phi_j(y)^\dagger \right|^2. \quad (18)$$

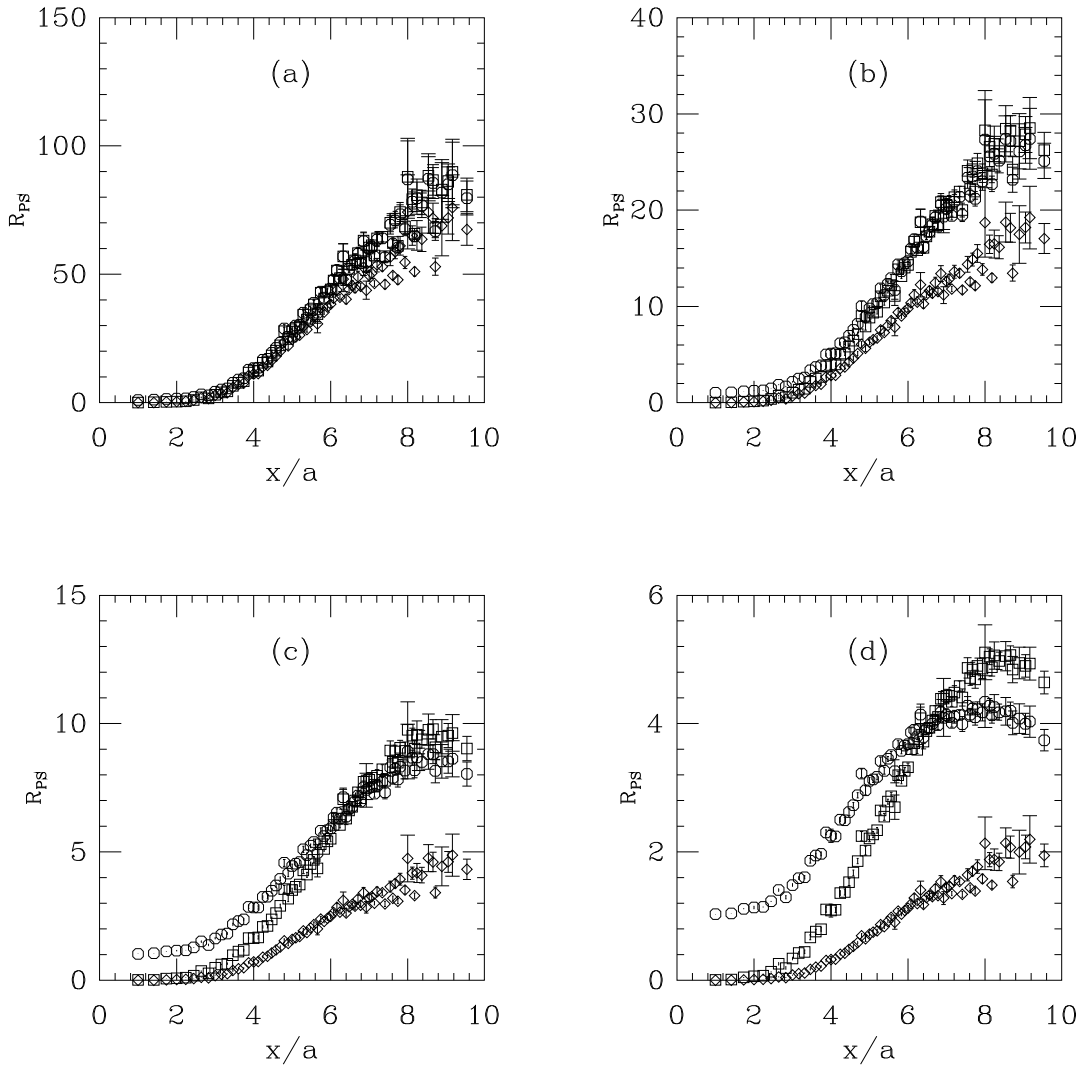


FIG. 1. Saturation of the point-to-point pseudoscalar correlator by low-lying eigenmodes of  $H(0)^2$ . (a)  $am_q = 0.01$  ( $m_{PS}/m_V \simeq 0.34$ ); (b)  $am_q = 0.02$  ( $m_{PS}/m_V \simeq 0.50$ ); (c)  $am_q = 0.04$  ( $m_{PS}/m_V \simeq 0.61$ ); (d)  $am_q = 0.06$  ( $m_{PS}/m_V \simeq 0.64$ ). Octagons show the full hadron correlator. Squares show the contribution from the lowest 10 modes. Diamonds show the contribution from the zero modes, which just scales as  $1/(am_q)^2$ .

As the quark mass rises, the approximation of  $R_{PS}(x)$  by a small number (ten) of low-lying eigenmodes becomes poorer and poorer. This is shown in Fig. 2. The correlators flatten and approach unity over a wide range of  $x$ . That the low eigenvalue modes do not saturate the correlator shows physics of these heavier pseudoscalars has little to do with fermion eigenmodes which are strongly coupled to instantons. This is not a surprise. It points up the dangerous possibility, however, that lattice simulations involving pseudoscalars performed at a pseudoscalar to vector ratio above 0.7 or so might give misleading results when extrapolated to small quark mass.

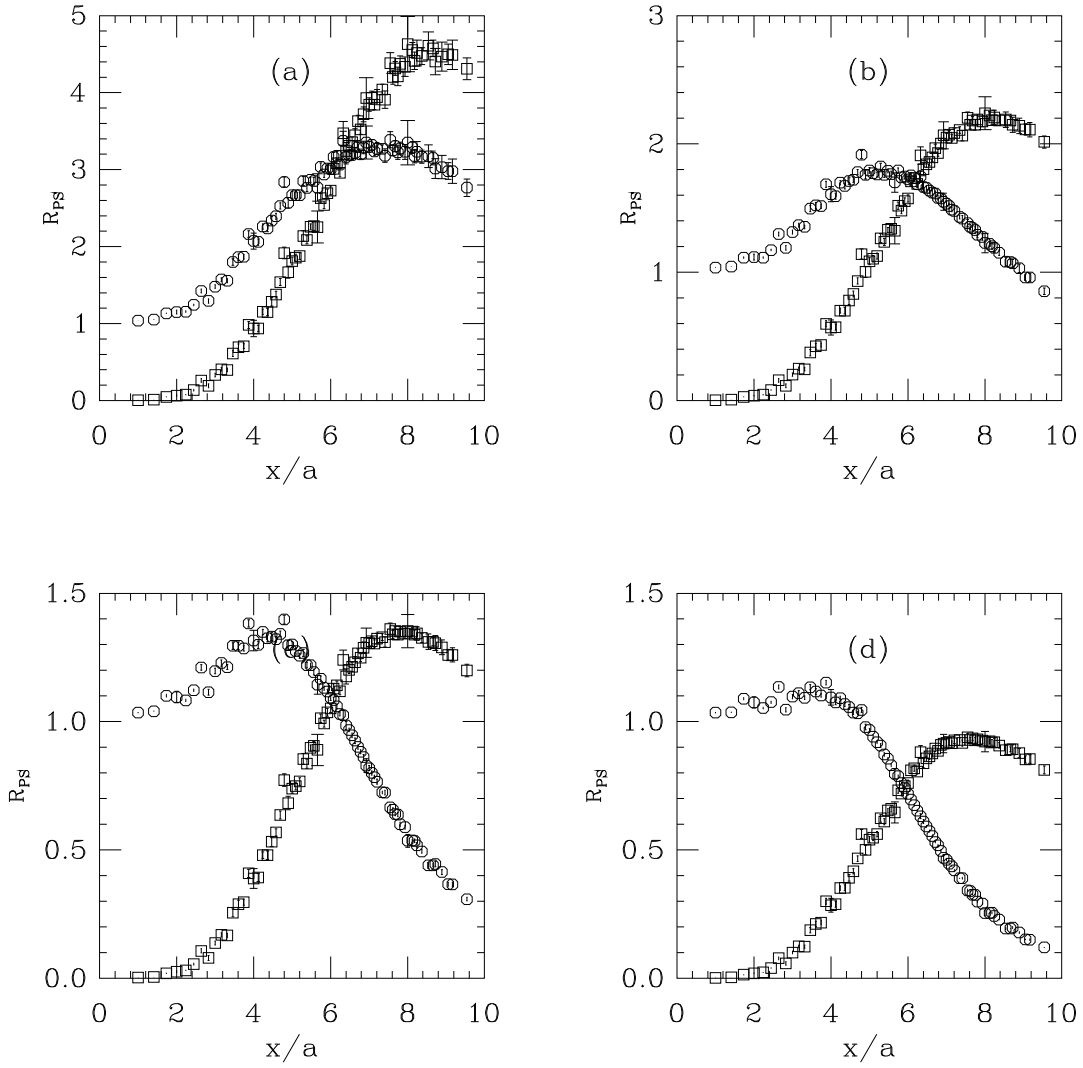


FIG. 2. Non-saturation of the point-to-point pseudoscalar correlator for heavier quark masses by low-lying eigenmodes of  $H(0)^2$ . (a)  $am_q = 0.10$  ( $m_{PS}/m_V \simeq 0.75$ ); (b)  $am_q = 0.15$  ( $m_{PS}/m_V \simeq 0.84$ ); (c)  $am_q = 0.20$  ( $m_{PS}/m_V \simeq 0.87$ ); (d)  $am_q = 0.25$  ( $m_{PS}/m_V \simeq 0.91$ ). Octagons show the full hadron correlator. Squares show the contribution from the lowest 10 modes.

The scalar correlator shows similar qualitative behavior to the pseudoscalar correlator: strong deviation from unity away from small  $x$  and at small quark mass a large contribution from zero modes. See Fig. 3.

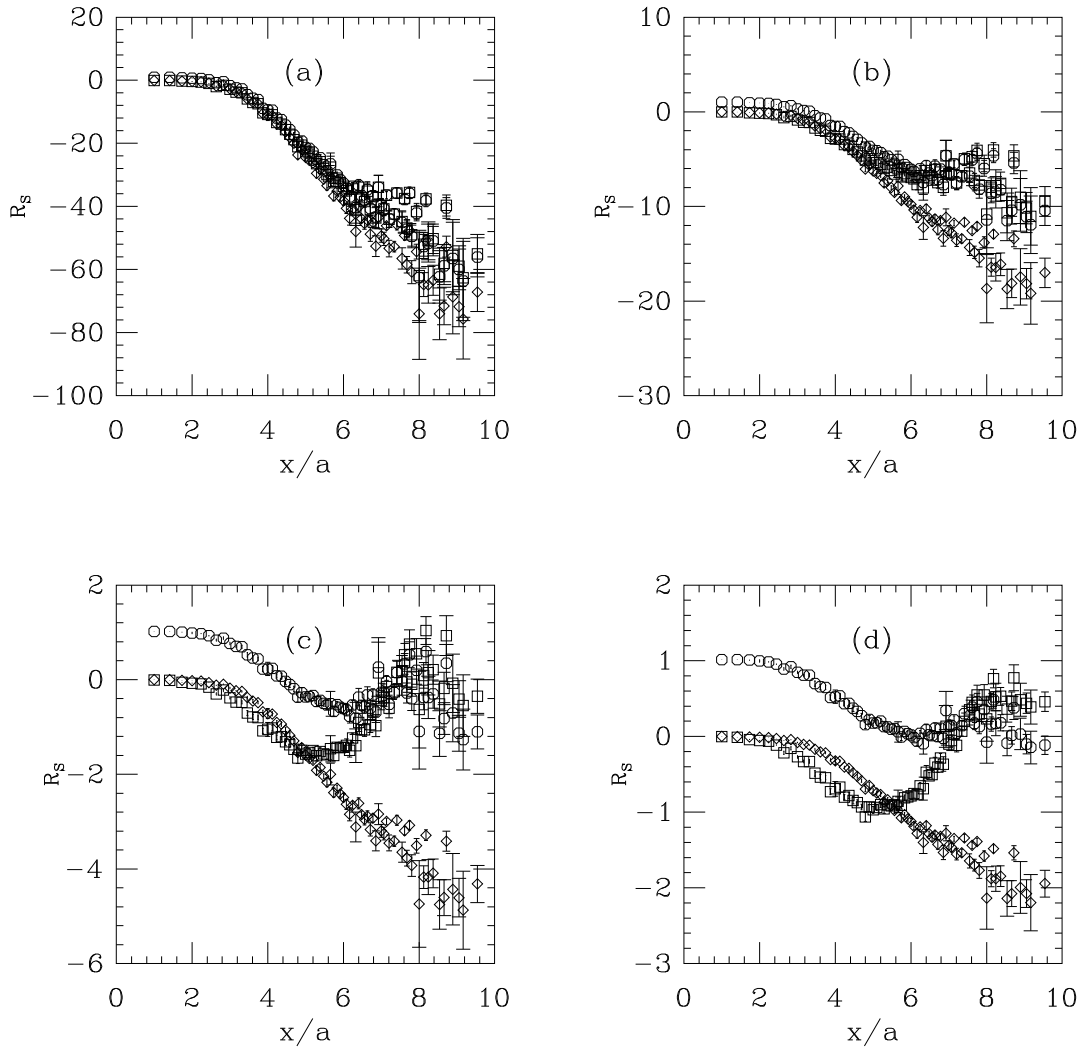


FIG. 3. Saturation of the point-to-point scalar correlator by low-lying eigenmodes of  $H(0)^2$ . (a)  $am_q = 0.01$  ( $m_{PS}/m_V \simeq 0.34$ ); (b)  $am_q = 0.02$  ( $m_{PS}/m_V \simeq 0.50$ ); (c)  $am_q = 0.04$  ( $m_{PS}/m_V \simeq 0.61$ ); (d)  $am_q = 0.06$  ( $m_{PS}/m_V \simeq 0.64$ ). Octagons show the full hadron correlator. Squares show the contribution from the lowest 10 modes. Diamonds show the contribution from the zero modes, which again just scales as  $1/(am_q)^2$ .

Instanton liquid models predict a repulsive interaction in this channel. We see that, indeed, the interaction between quarks is strongly repulsive – so strongly repulsive, that at small quark mass, the correlator becomes negative at larger  $x$ .

The bulk of this effect is due to the zero modes. To make the argument, I begin by considering the susceptibilities, or spatial integrals of the correlators [22]: In the pseudoscalar channel, configuration by configuration, if the configuration has topological charge  $Q$ ,

$$\chi_\pi = \frac{1}{V} \sum_{x,y,a} \langle J_{PS}^a(x) J_{PS}^a(y) \rangle = \frac{2}{V} \text{Tr} (\hat{D}^{-1} \gamma_5)^2 \quad (19)$$

$$= 2 \frac{|Q|}{m^2 V} + \frac{4}{V} \sum_j (\beta_j^2 + \alpha_j^2) \quad (20)$$

$$= \frac{2}{m} \langle \bar{\psi} \psi \rangle \quad (21)$$

The last line is the Gell-Mann, Oakes, Renner relation, which is satisfied exactly by overlap fermions. The isotriplet scalar susceptibility is



$$\chi_{a_0} = \frac{1}{V} \sum_{x,y,a} \langle J_S^a(x) J_S^a(y) \rangle = -\frac{2}{V} \text{Tr } \hat{D}^{-2} \quad (22)$$

$$= -2 \frac{|Q|}{m^2 V} + \frac{4}{V} \sum_j (\beta_j^2 - \alpha_j^2). \quad (23)$$

Note the negative contribution of the zero modes to the scalar channel. In general, one would expect the sum over the nonzero modes to contribute a result of order unity to the susceptibility. The contribution of the zero modes should scale away as  $1/\sqrt{V}$ , since the existence of a topological susceptibility means that  $\langle Q^2 \rangle \simeq V$ . Thus the zero mode contribution to both the pseudoscalar and scalar channels is a finite volume artifact, but one which dies away quite slowly.

So much for the integral of the correlator; what about its value point by point? The contributions where both of the quark lines propagate through zero modes are equal in magnitude and opposite in sign in the pseudoscalar and scalar channels. If the correlator is dominated by modes whose eigenvalues are large compared to the quark mass, one would expect the nonzero mode sum to contribute positively to the correlator. This is certainly the case for the free theory, and so we naturally have a situation where the free scalar correlator is positive and the interacting correlator is dominated by its zero modes and is negative.

One can check that the zero mode is the source of the loss of spectral positivity by considering the scalar propagator in the subset of our lattices which have zero topological charge (5 of the 20 lattices). This is shown in Fig. 4. Notice that the scalar correlator in this sector is still saturated by low eigenmodes of the Dirac operator for  $m_{PS}/m_V \leq 0.5$  at a distance of 5 lattice spacings ( $x \simeq 0.55$  fm). In this sector the channel only becomes strongly repulsive at heavier quark masses, where the low modes do not contribute to the correlator.

The  $Q = 0$  sector of QCD is not QCD and so it remains an open question, what will happen at larger volumes.

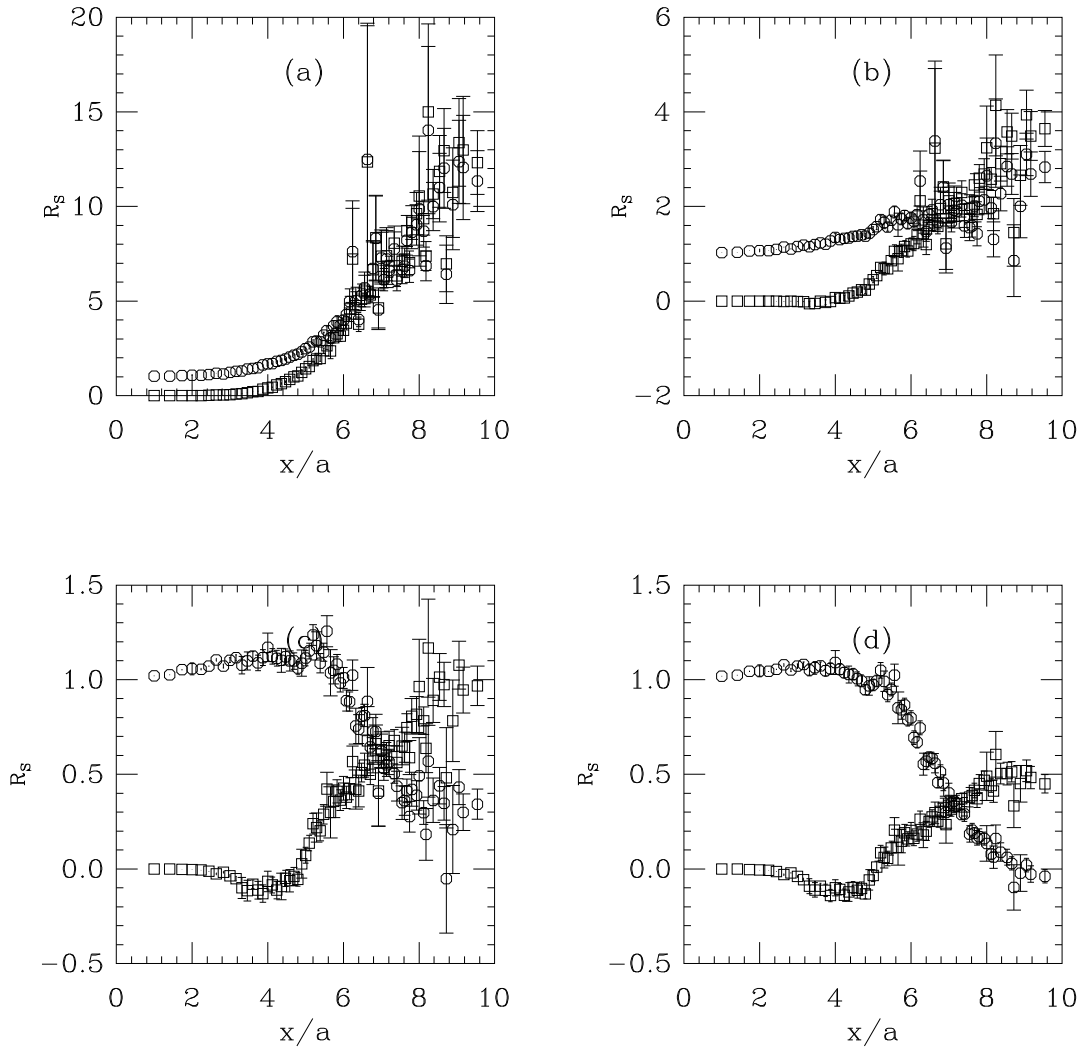


FIG. 4. Comparison of the point-to-point scalar correlator to the scalar correlator composed of low-eigenvalue quark modes in the  $Q = 0$  sector. (a)  $am_q = 0.01$  ( $m_{PS}/m_V \simeq 0.34$ ); (b)  $am_q = 0.02$  ( $m_{PS}/m_V \simeq 0.50$ ); (c)  $am_q = 0.04$  ( $m_{PS}/m_V \simeq 0.61$ ); (d)  $am_q = 0.06$  ( $m_{PS}/m_V \simeq 0.64$ ). Octagons show the full hadron correlator. Squares show the contribution from the lowest 10 modes.

Finally, one might worry that all of the attraction in the pseudoscalar channel is due to the zero modes. The sum of pseudoscalar and scalar correlators,

$$R_{PS+S}(x) = \frac{\Pi_{PS}(x) + \Pi_S(x)}{2\Pi_{PS}^0(x)}. \quad (24)$$

has no zero mode contribution.

This quantity is shown in Fig. 5. The low modes do not contribute to the correlator at small  $x$ . At larger  $x$  they show a significant attractive interaction, saturating the full-propagator correlator at larger  $x$  for  $m_{PS}/m_V \leq 0.5$ . At heavier masses they produce too much attraction at larger  $x$ .

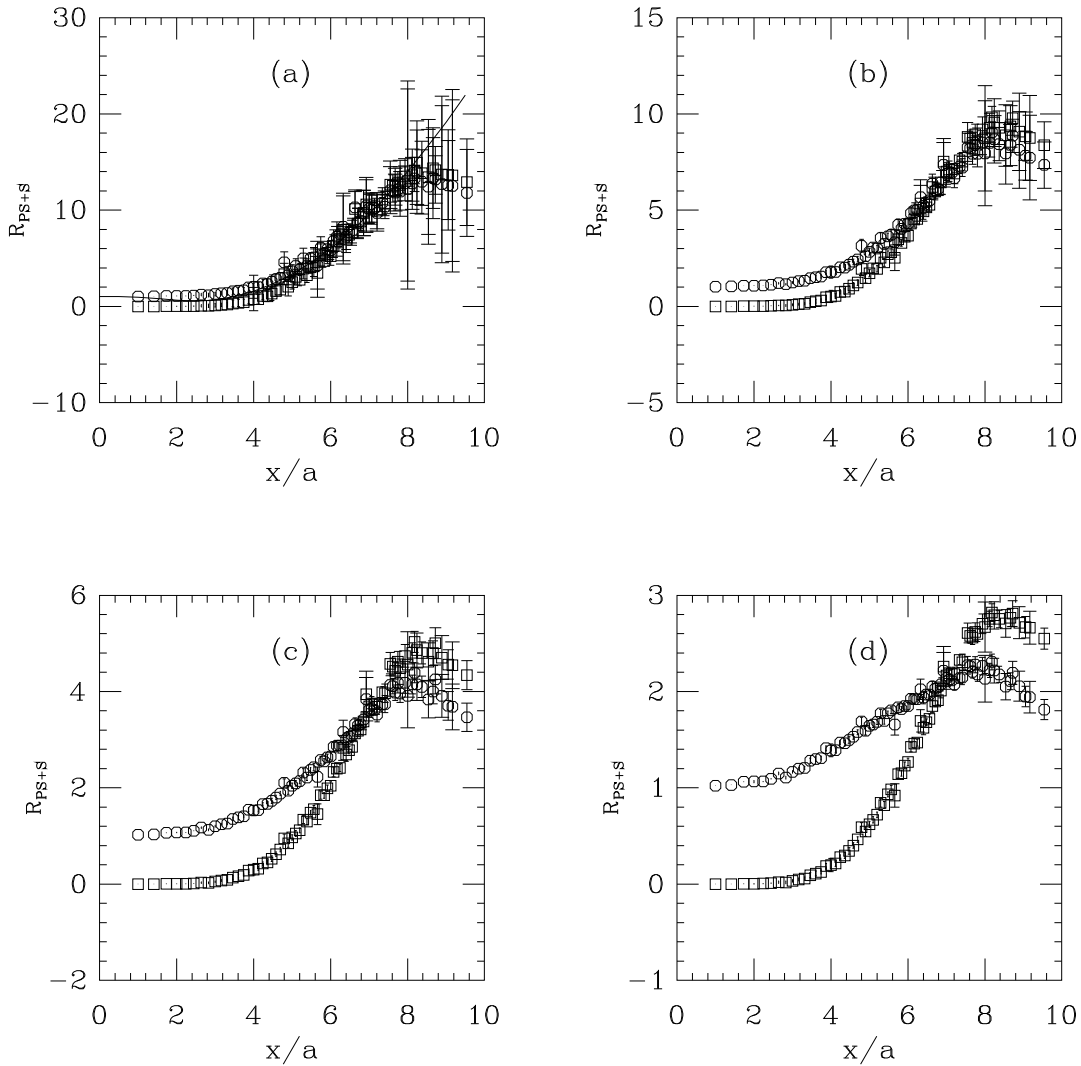


FIG. 5. Saturation of the sum of point-to-point pseudoscalar and scalar correlators sector by low-lying eigenmodes of  $H(0)^2$ . (a)  $am_q = 0.01$  ( $m_{PS}/m_V \simeq 0.34$ ); (b)  $am_q = 0.02$  ( $m_{PS}/m_V \simeq 0.50$ ); (c)  $am_q = 0.04$  ( $m_{PS}/m_V \simeq 0.61$ ); (d)  $am_q = 0.06$  ( $m_{PS}/m_V \simeq 0.64$ ). Octagons show the full hadron correlator. Squares show the contribution from the lowest 10 modes. The curve in panel (a) is from a simple phenomenological parameterization of the spectral density.

Other possibilities for a negative spectral weight could exist in the scalar channel. Schafer and Shuryak [27] actually show that the scalar correlator in interacting instanton models becomes negative at  $x \simeq 0.5$  fm. They ascribe this behavior to the strong repulsion in the scalar channel expected in instanton models becoming a little too strong, and their calculations of interacting instantons which include dynamical fermion effects soften the interaction and restore positivity.

Recently, a discussion of the same effect has been given by Thacker *et al* [28] in the context of quenched chiral perturbation theory [29]: In full QCD the quark and antiquarks in the eta-prime, the flavor singlet pseudoscalar meson, can annihilate and the (multi)  $q\bar{q}$  pair(s) Fock state of the meson can mix with a quarkless intermediate state. This mixing shifts the mass of the eta-prime. In the quenched approximation the sum of mixing graphs truncates with a single term and the propagator consists of a single pole and a double pole with a negative coefficient, a ghost.

$$G(p) = \frac{1}{p^2 + m^2} - \frac{1}{p^2 + m^2} \frac{\mu^2}{3} \frac{1}{p^2 + m^2} \quad (25)$$

A negative spectral weight in the scalar channel can appear because the scalar particle can couple to an intermediate state which is a combination of a pion and a quenched eta-prime, whose propagator is the second term (hairpin) part of Eq. 25. This is a connected graph so in the quenched approximation it can be constructed. It is shown in Fig. 6.

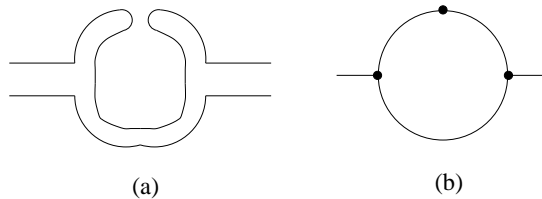


FIG. 6. The quark line graph (a) and associated Feynman graph (b) which makes a ghost contribution to the scalar correlator.

While we do not know the overall magnitude of the graph, the particle in all the propagators is the flavor nonsinglet pseudoscalar, whose mass is known from conventional spectroscopy calculations. If I assume that the scalar particle-pion-eta coupling is just a scalar constant  $g$ , then I can compute  $\rho(s)$  from the graph of Fig.6(b). Because of the minus sign in Eq. 25 the amplitude is negative and it is also divergent at threshold,

$$\rho(s) = -\frac{\mu^2 g^2}{\sqrt{s(s - 4m_\pi^2)}}. \quad (26)$$

Then the shape of  $R(x)$  can be computed exactly up to an overall normalization. This contribution can have nothing to do with the zero modes because the spatial correlations of the zero modes do not depend on the quark mass. Attempts to fit the lattice data of Fig. 3 to a conventional [5] combination of continuum-like background  $\rho(s) = (3s/(8\pi^2))\theta(s - s_0)$  plus a possible scalar resonance plus the ghost term (even varying the strength of the ghost coupling with quark mass) were unsuccessful.

Schäfer and Shuryak have presented predictions for point to point correlators in the instanton liquid model. It would be an interesting exercise to compare lattice results to theirs. Because of the presence of the zero mode contribution in the pseudoscalar and scalar channels, it probably makes the most sense to consider the sum of pseudoscalar and scalar channels, from which the zero modes decouple. Next, one must choose a lattice spacing. Because the correlators rise up so strongly with  $x$ , they are very sensitive to the choice of lattice spacing. I have collected a number of observables for this simulation, which happen to have more or less well-known continuum values, and which might be used to infer a lattice spacing, in Table I. The quantity  $r_0$  is the Sommer parameter, from Ref. [23]. The rho mass, pseudoscalar decay constant, and pseudoscalar matrix element  $\lambda_\pi = \langle 0|\bar{\psi}\gamma_5\psi|PS\rangle$  (all extrapolated to zero quark mass) are determined from simulations on  $12^3 \times 24$  lattices at the same parameter values [9], while the infinite volume  $\Sigma$  measurement is from Ref. [10]. The phenomenological estimate for  $\lambda_\pi$ , which is equal to  $f_\pi m_\pi^2/(m_u + m_d)$ , is from Ref. [5]. The inferred lattice spacing, shown in the fourth column of the Table, includes the unknown (but believed to be close to unity) lattice-to-continuum renormalization factors appropriate to each observable.

The dominant feature of  $R_{PS}(x)$  or  $R_{PS+S}(x)$  is the pion. Its contribution is proportional to  $\lambda_\pi^2$ , or to the fourth power of the lattice spacing. This is the source of the sensitivity of the correlator to  $a$ .

quantity	lattice value	continuum	lattice spacing (fm)
$r_0$	see [23]	0.5 fm	0.11
$m_\rho$	$am_\rho = 0.50(2)$	770 MeV	0.13
$f_\pi$	$af_\pi = 0.078(1)$	131 MeV	$0.12/Z_A$
$\lambda_\pi$	$a^2\lambda_\pi = 0.143(3)$	$(470 \text{ MeV})^2$	$0.16 Z_A Z_m$
$\langle\bar{\psi}\psi\rangle$	$a^3\Sigma = 0.0039(1)$	$(250 \text{ MeV})^3$	$0.13 Z_m^{1/3}$

TABLE I. Table of observables and inferred lattice spacings.

I will somewhat arbitrarily take the lattice spacing to be 0.13 fm in Fig. 7, where I compare the lattice results to instanton liquid model data from Ref. [27]. The solid line is a very naive phenomenological calculation of  $R_{PS+S}$ : I take a spectral function which has a delta-function pion of weight  $\lambda_\pi^2/2$  (with its value from the Table) and add in a step function representing a continuum:  $\rho_{cont}(x) \simeq \theta(s - s_0)$  with  $s_0 = 0.5 \text{ GeV}^2$ . This parameterization does a very good job of modeling the low quark mass lattice data, when one inputs the observed lattice values of pseudoscalar mass and  $\lambda_\pi$ , as is shown in panel (a) of Fig. 5. In Fig. 7 the data overshoots the model by about thirty per cent. It will take simulations at a smaller lattice spacing to disentangle scale violations from lattice spacing uncertainties, to improve this picture.

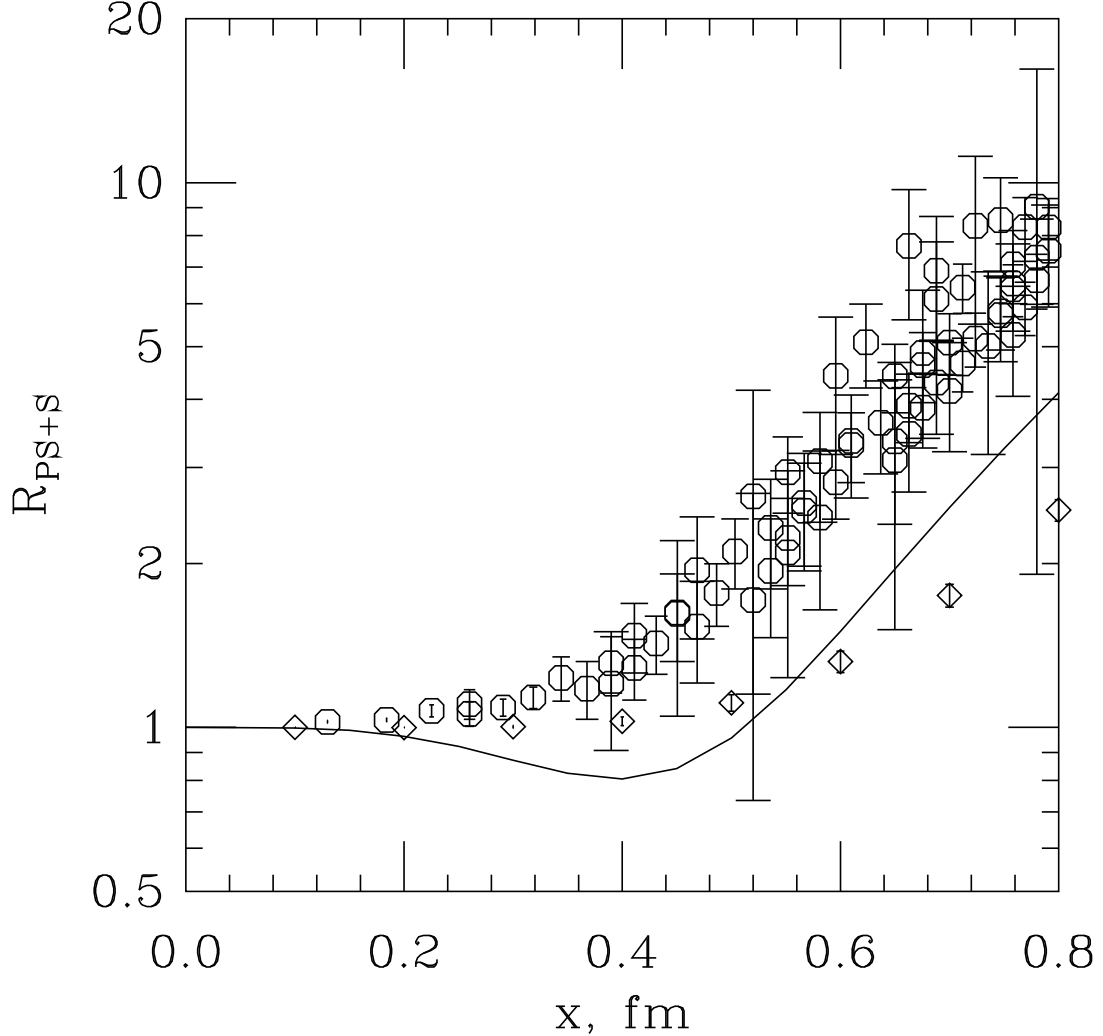


FIG. 7. Comparison of the sum of lattice point-to-point pseudoscalar and scalar correlators, extrapolated to zero quark mass (octagons), predictions of the instanton liquid model (diamonds) and a simple phenomenological model for  $\rho(s)$  (solid line).

### B. The vector and axial vector channels

The potentially interesting physics in these channels involves a comparison of lattice data to the predictions of the OPE. With my sign conventions, the coordinate-space quark propagator (with flavor label  $a, b$  in slowly varying external fields is (for references see [3])

$$S(x)^{ab} = \frac{\delta^{ab}}{2\pi^2} \frac{\gamma \cdot x}{x^4} + \frac{\delta^{ab}}{4\pi^2} \frac{m}{x^2} + q^a(0)\bar{q}^b(0) + \frac{G''}{x^2} + \dots \quad (27)$$

where the rather schematic “ $G/x^2$ ” represents a long expression which will give the gluon condensate term in a mesonic correlator. With this quark propagator all the quark mass and quark condensate dependence in the “sum”  $R_{V+A}$  correlator cancels out, while the “difference” correlator for massive quarks is

$$R_{V-A} = \frac{m^2 x^2}{2} + m\pi^2 \langle \bar{q}q \rangle x^4 + Ax^6 + \dots \quad (28)$$

and the  $Ax^6$  term is  $Ax^6 = (\pi^3/9)\alpha_s(x)\langle \bar{q}q \rangle^2 x^6$  which is estimated by Schäfer and Shuryak to be about  $(x/0.66 \text{ fm})^6$ . The “sum” correlator sees the gluon condensate

$$R_{V+A} = 1 + \frac{\alpha_s(x)}{\pi} - \frac{1}{384} \langle g^2 (G_{\mu\nu}^a)^2 \rangle x^4 + \frac{2\pi^3}{81} \alpha_s(x) \langle \bar{q}q \rangle \log(x^2) x^6 + \dots \quad (29)$$

Figs. 8 and 9 show  $R_{V\pm A}$  correlators from the full simulation and from the lowest ten eigenmodes. The low modes clearly saturate the “difference” correlator at  $m_{PS}/m_V \leq 0.5$ . The “sum” correlator is essentially unity, and receives little contribution from the low eigenmodes.

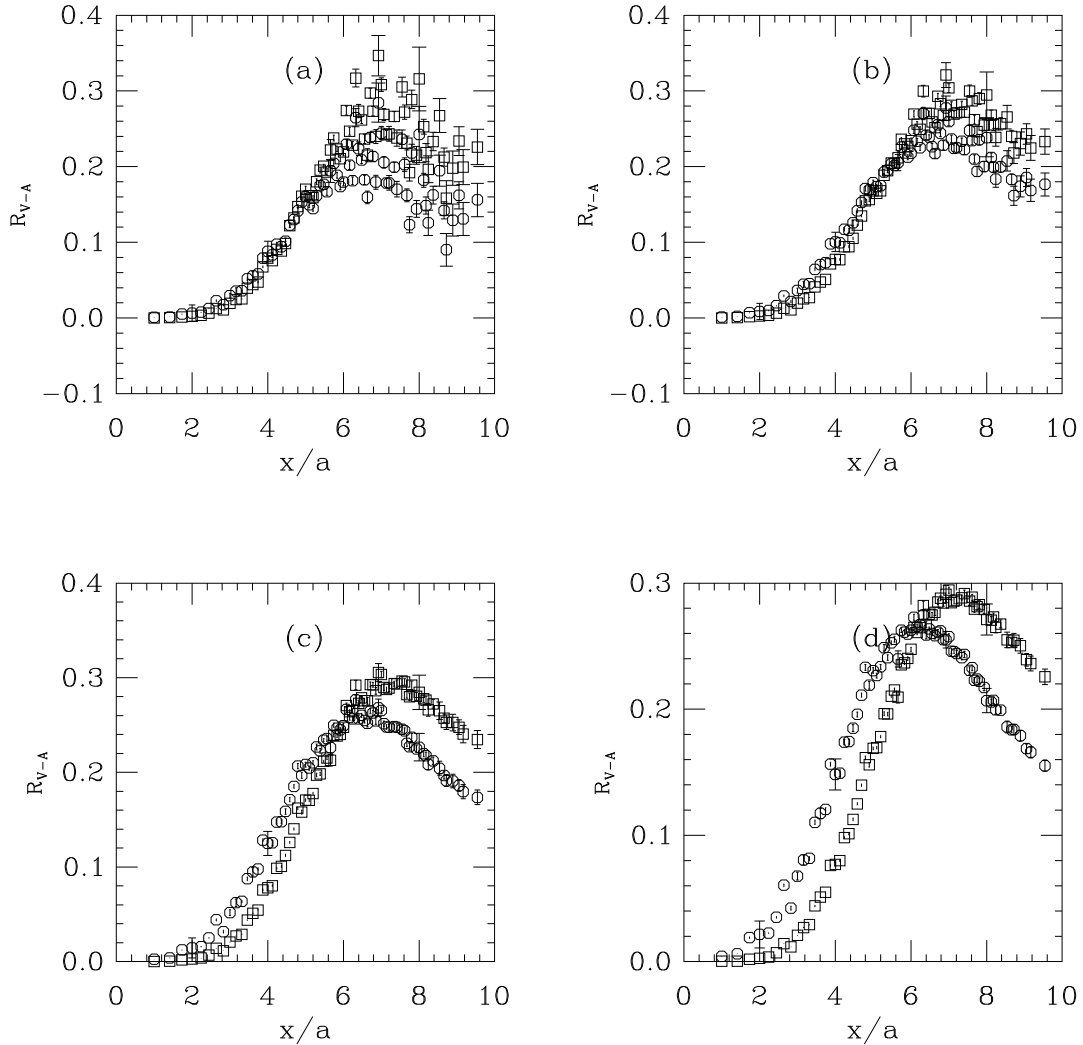


FIG. 8. Saturation of the difference of point-to-point vector minus axial correlators by low-lying eigenmodes of  $H(0)^2$ . (a)  $am_q = 0.01$  ( $m_{PS}/m_V \simeq 0.34$ ); (b)  $am_q = 0.02$  ( $m_{PS}/m_V \simeq 0.50$ ); (c)  $am_q = 0.04$  ( $m_{PS}/m_V \simeq 0.61$ ); (d)  $am_q = 0.06$  ( $m_{PS}/m_V \simeq 0.64$ ). Octagons show the full hadron correlator. Squares show the contribution from the lowest 10 modes.

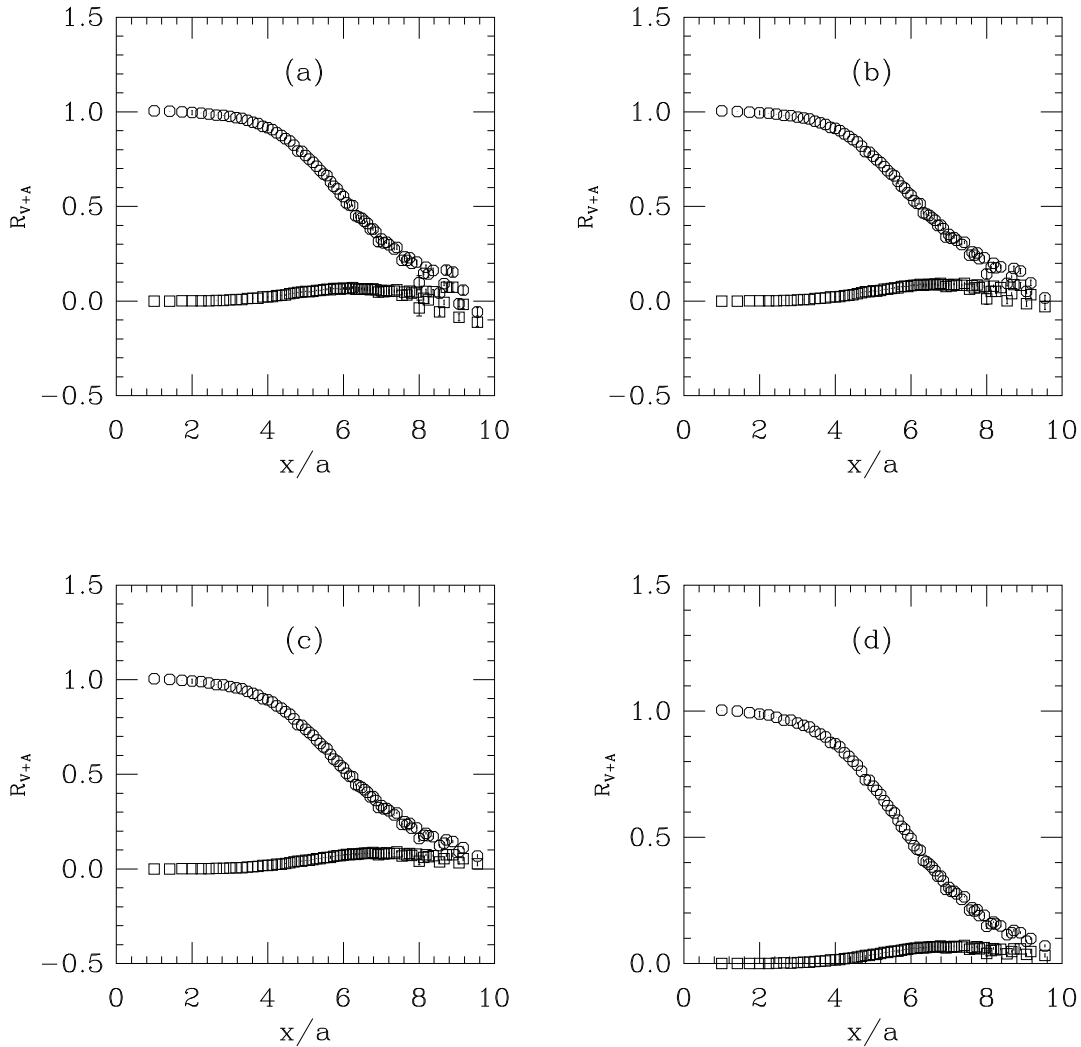


FIG. 9. Comparison of the summed point-to-point vector and axial vector correlators from the full quark propagator and with the propagator built of low-lying eigenmodes of  $H(0)^2$ . (a)  $am_q = 0.01$  ( $m_{PS}/m_V \simeq 0.34$ ); (b)  $am_q = 0.02$  ( $m_{PS}/m_V \simeq 0.50$ ); (c)  $am_q = 0.04$  ( $m_{PS}/m_V \simeq 0.61$ ); (d)  $am_q = 0.06$  ( $m_{PS}/m_V \simeq 0.64$ ). Octagons show the full hadron correlator. Squares show the contribution from the lowest 10 modes.

Now the lattice data is collected at several values of quark mass, all of which are greater than the physical quark mass, and so to make connection with phenomenology it is necessary to extrapolate all the data to zero quark mass. The extrapolation itself can shed light on the OPE prediction: I will assume that point-by-point in  $x$ ,  $R(x) = r_0 + r_1 m_q + r_2 m_q^2$ . For both correlators, the mass dependence is weak and the extrapolation is readily performed. However, the coefficients of  $m_q$  and  $m_q^2$  expected from the OPE, Eq. 28, are only seen at very low  $x$ ,  $x/a < 4$ .

The extrapolated data can be compared to non-lattice results. Figs. 10 and 11 show the lattice correlators with the instanton model of Ref. [8] (crosses) and ALEPH  $\tau$ -lepton decay, as extracted by Ref. [8] (lines). In these figures I have re-introduced a physical distance scale (in fm) for the separation  $x$  by using the same lattice spacing (0.13 fm, from the rho mass) as used in the last section. Because the correlator is such a flat function of  $x$ , it is not too sensitive to the choice of lattice spacing.

Lattice Monte Carlo data, the instanton liquid model, and the extracted tau decay data for  $R_{V-A}$  all agree nicely. This is a channel which has no short distance contributions, and the long distance contributions are dominated by instanton-sensitive eigenmodes.

The lattice data for  $R_{V+A}$  also agree with the instanton liquid model out to a distance of about 0.6 fm, and then become less attractive. They undershoot the tau decay data by about five cent. It is plausible to assume that the latter discrepancy is just due to the lack of lattice physics below the cutoff scale, and to the fat link used in the gluon vertex, which smears the action out to about two lattice spacings (0.26 fm, nominally). It is the same discrepancy as the instanton liquid model data, which does not “naturally” include the perturbative  $\alpha_s/\pi$  part of the correlator. Of

course, as I have remarked earlier, I have not computed the lattice to continuum conversion factor for the vector and axial currents. While it is unlikely to account for all the discrepancy, it might be the source of some of it.

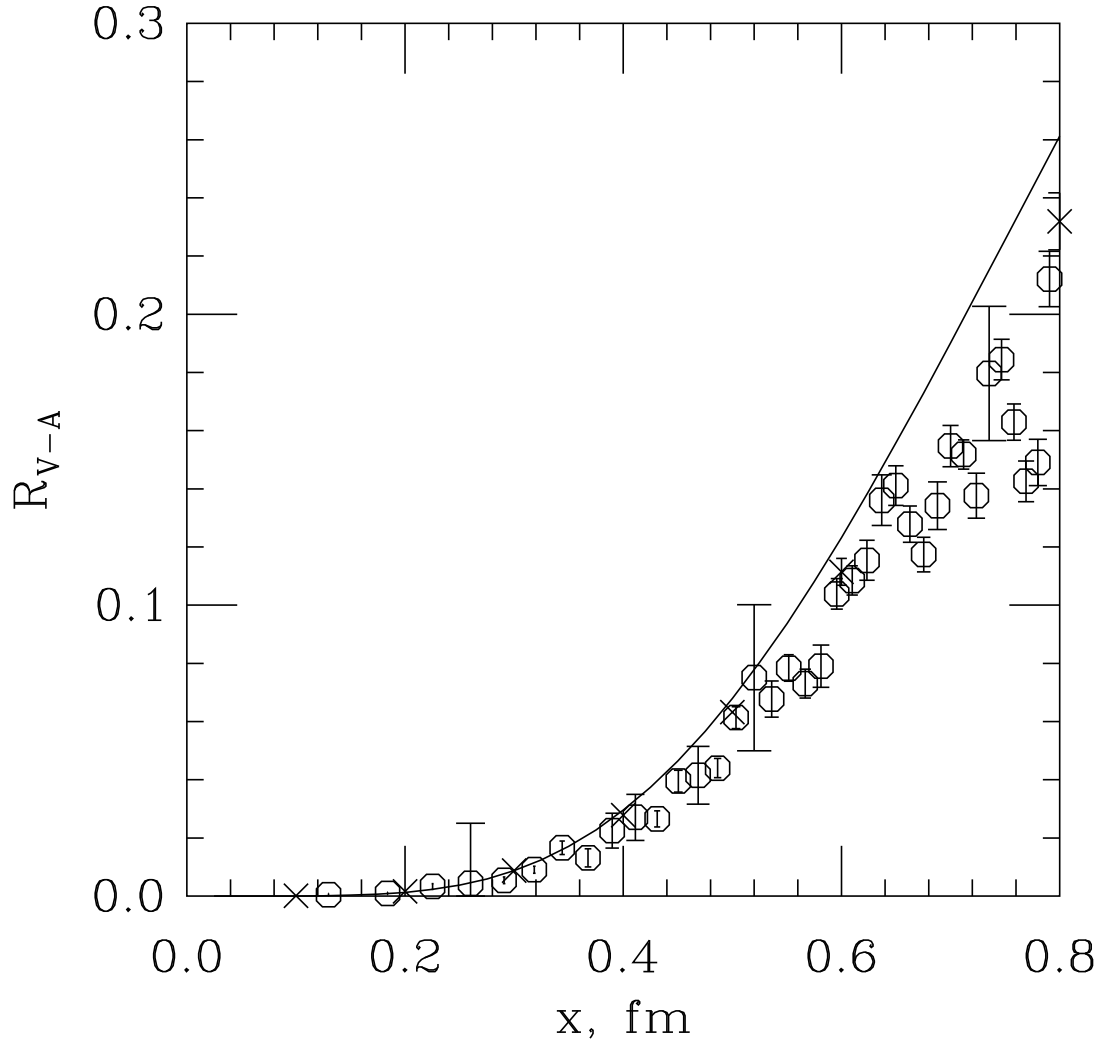


FIG. 10. Comparison of the difference point-to-point vector and axial vector correlators from the overlap action (octagons), extrapolated to zero quark mass, and from the instanton model of Ref. [8] (crosses) and ALEPH  $\tau$ -lepton decay, as extracted by Ref. [8] (lines).



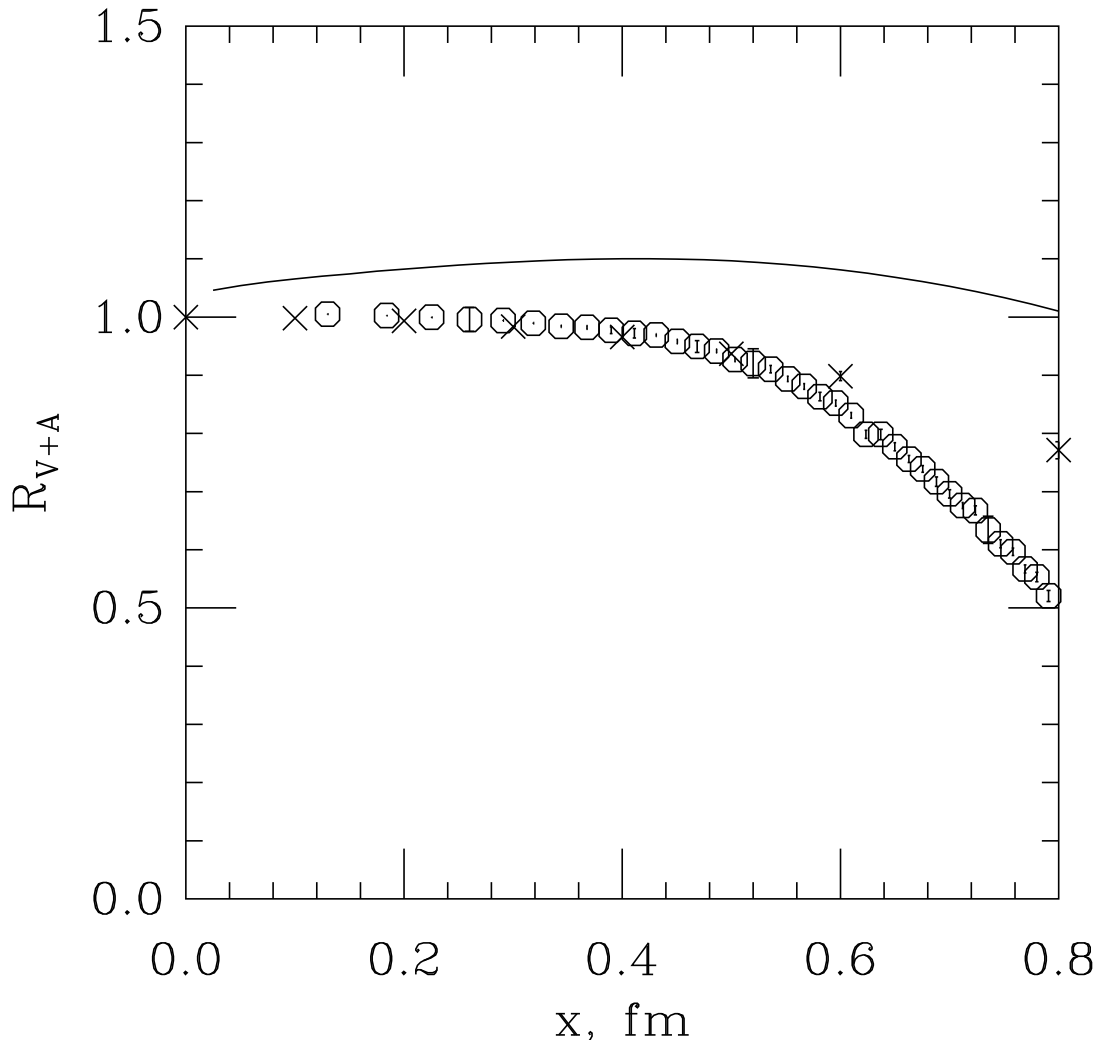


FIG. 11. Comparison of the sum of point-to-point vector and axial vector correlators from the overlap action (octagons), extrapolated to zero quark mass, and from the instanton model of Ref. [8] (crosses) and ALEPH  $\tau$ -lepton decay, as extracted by Ref. [8] (lines).

The authors of Ref. [8] perform fits to  $R_{V\pm A}(x)$  in order to extract the various condensate terms (which will appear as different powers of  $x^n$ ), as well as to look for  $\log x^2$  terms so characteristic of the operator product expansion. I tried to do this with the lattice data. Because the lattice data and instanton liquid model data are so similar, the results will be similar to those found in Ref. [8]—that is, difficult to reconcile with the OPE.

For example, consider  $R_{V-A}$ . The action itself has order  $a^2$  discretization errors, which generate terms in  $R(x)$  proportional to  $x^2$ . Good fits to the lattice data can be found beginning with any even power of  $x$ . However, if we take the continuum theory seriously and consider only fits beginning with  $x^6$  term, one can find fits for  $x < 0.4$  fm or so of the form  $(x/0.6 \text{ fm})^6$ , quite close to the expectation of the OPE and the results of Schäfer and Shuryak [27].

Fits to  $R_{V+A}$  designed to expose the gluon condensate term are also not very successful. The fit parameters are quite sensitive to the range of  $x$ . Most fits (which range from 0.11 to 0.4 fm or so) give a far too large condensate term and the wrong sign for the  $x^6$  term.

#### IV. CONCLUSIONS

Low-lying eigenmodes of the Dirac operator, which we have previously argued in Ref. [9] couple strongly to instantons and anti-instantons, dominate the nonperturbative part of short distance correlators for light quark masses in the pseudoscalar, scalar, vector and axial vector channels. In the pseudoscalar channel they are responsible for the bulk of the observed strong attraction. The zero eigenmodes in the scalar channel contribute a strong repulsion at larger

distances. The pseudoscalar plus scalar channel is more attractive on the lattice than in the instanton liquid model. The low modes dominate the vector minus axial vector channel, which has no perturbative contribution. The lattice calculations quantitatively reproduce the results of instanton liquid models in the sum and difference of vector and axial vector channels. The difference between the lattice results and correlation function extracted from tau data in the  $V + A$  channel can plausibly be attributed to short distance physics. As the quark mass rises, the relative importance of the light modes decreases in all observed channels.

The lattice simulations could be done much better. It seems to me that these simulations are rather more sensitive to systematic effects than they are to statistics. Since one is comparing results to free field theory, an overlap action with better “kinetic” (dispersion relation, rotational invariance) properties might be a better choice [30]. Even though these correlators are called “short distance,” a larger volume is needed to suppress zero mode effects and to deal with the weak (power law) falloff of the normalizing free correlators. (A nonchiral action would be cheaper to simulate, but would suffer from fatal exceptional configurations at the low values of quark masses needed to study interesting physics questions.) Finally, if one wants to look for OPE terms in the correlators it will be necessary to drop the lattice spacing and convert to links which smear only a minimal distance—the hypercubic blocking of Hasenfratz and Knechtli [31] would be a good choice. It seems to me since most of the physics which is being explored here involves chiral symmetry, it would be a mistake to look at these correlators with a nonchiral lattice action.

With the use of a chiral fermion action, lattice calculations may be poised to say more interesting things about spectral functions in QCD.

### ACKNOWLEDGEMENTS

This work was supported by the U. S. Department of Energy. I would like to thank A. Hasenfratz for numerous conversations, and E. Shuryak and T. Schäfer for much valuable correspondence and for providing me with tables of their data.

- 
- [1] M. A. Shifman, A. I. Vainshtein and V. I. Zakharov, Nucl. Phys. B **147**, 385 (1979); Nucl. Phys. B **147**, 448 (1979).
  - [2] For reviews, cf. M. Shifman, Prog. Theor. Phys. Suppl. **131**, 1 (1998) [hep-ph/9802214]; hep-ph/0009131; P. Colangelo and A. Khodjamirian, hep-ph/0010175.
  - [3] T. Schafer and E. V. Shuryak, Rev. Mod. Phys. **70**, 323 (1998) [hep-ph/9610451].
  - [4] D. Diakanov, Lectures at the Enrico Fermi School in Physics, Varenna, 1995 [hep-ph/9602375]
  - [5] E. V. Shuryak, Rev. Mod. Phys. **65**, 1 (1993).
  - [6] P. H. Ginsparg and K. G. Wilson, Phys. Rev. **D25**, 2649 (1982).
  - [7] H. Neuberger, Phys. Lett. **B417**, 141 (1998) [hep-lat/9707022], Phys. Rev. Lett. **81**, 4060 (1998) [hep-lat/9806025].
  - [8] T. Schafer and E. V. Shuryak, Phys. Rev. Lett. **86**, 3973 (2001) [hep-ph/0010116].
  - [9] T. DeGrand and A. Hasenfratz, Phys. Rev. D, in press; hep-lat/0012021.
  - [10] T. DeGrand [MILC collaboration], Phys. Rev. D **63**, 034503 (2001) [hep-lat/0007046].
  - [11] I. Horvath, N. Isgur, J. McCune and H. B. Thacker, hep-lat/0102003.
  - [12] T. DeGrand and A. Hasenfratz, charge fluctuations in QCD,” hep-lat/0103002.
  - [13] R. G. Edwards and U. M. Heller, hep-lat/0105004.
  - [14] T. Blum *et al.*, hep-lat/0105006.
  - [15] C. Gattringer, M. Goekeler, P. E. Rakow, S. Schaefer and A. Schaefer, hep-lat/0105023.
  - [16] I. Hip, T. Lippert, H. Neff, K. Schilling and W. Schroers, hep-lat/0105001.
  - [17] M. C. Chu, J. M. Grandy, S. Huang and J. W. Negele, Phys. Rev. D **48**, 3340 (1993) [hep-lat/9306002].
  - [18] S. J. Hands, P. W. Stephenson and A. McKerrell [UKQCD Collaboration], Phys. Rev. D **51**, 6394 (1995) [hep-lat/9412065].
  - [19] T. L. Ivanenko and J. W. Negele, Nucl. Phys. Proc. Suppl. **63**, 504 (1998) [hep-lat/9709130]; R. C. Brower, T. L. Ivanenko, J. W. Negele and K. N. Orginos, Nucl. Phys. Proc. Suppl. **53**, 547 (1997) [hep-lat/9608086]; T. L. Ivanenko, MIT thesis (unpublished, 1997).
  - [20] M. Albanese *et al.* [APE Collaboration], Phys. Lett. **B192**, 163 (1987); M. Falcioni, M. L. Paciello, G. Parisi and B. Taglienti, Nucl. Phys. **B251** (1985) 624.
  - [21] See B. Bunk, K. Jansen, M. Lüscher, and H. Simma, unpublished DESY report (1994); T. Kalkreuter and H. Simma, Comput. Phys. Commun. **93**, 33 (1996) [hep-lat/9507023].
  - [22] R. G. Edwards, U. M. Heller and R. Narayanan, Phys. Rev. D **59**, 094510 (1999) [hep-lat/9811030].
  - [23] M. Guagnelli, R. Sommer and H. Wittig [ALPHA collaboration], Nucl. Phys. **B535**, 389 (1998) [hep-lat/9806005].

- [24] C. Bernard and T. DeGrand, Nucl. Phys. Proc. Suppl. **83-84**, 845 (2000) [hep-lat/9909083].
- [25] H. Leutwyler and A. Smilga, Phys. Rev. D **46**, 5607 (1992).
- [26] V. A. Novikov, M. A. Shifman, A. I. Vainshtein and V. I. Zakharov, Nucl. Phys. B **191**, 301 (1981).
- [27] T. Schafer and E. V. Shuryak, Phys. Rev. D **54**, 1099 (1996) [hep-ph/9512384].
- [28] H. B. Thacker, hep-lat/0011016; W. Bardeen, A. Duncan, E. Eichten, N. Isgur and H. Thacker, hep-lat/0106008.
- [29] Cf. S. R. Sharpe, Phys. Rev. D **46**, 3146 (1992) [hep-lat/9205020]; C. W. Bernard and M. F. Golterman, Phys. Rev. D **46**, 853 (1992) [hep-lat/9204007]; C. Bernard, M. Golterman, J. Labrenz, S. Sharpe and A. Ukawa, Nucl. Phys. Proc. Suppl. **34**, 334 (1994); C. W. Bernard and M. F. Golterman, Phys. Rev. D **53**, 476 (1996) [hep-lat/9507004].
- [30] Compare T. DeGrand [MILC Collaboration], Phys. Rev. D **58**, 094503 (1998) [hep-lat/9802012]; Phys. Rev. D **60**, 094501 (1999) [hep-lat/9903006]; P. Hasenfratz, S. Hauswirth, K. Holland, T. Jorg, F. Niedermayer and U. Wenger, hep-lat/0003013; Nucl. Phys. Proc. Suppl. **94**, 627 (2001) [hep-lat/0010061].
- [31] A. Hasenfratz and F. Knechtli, Phys. Rev. D **64**, 034504 (2001) [hep-lat/0103029].